Anistropic exchange interactions in CuGeO3 probed by electron spin resonance spectroscopy

R. M. Eremina, Mikhail V. Eremin, V. N. Glazkov, Hans-Albrecht Krug von Nidda, Alois Loidl

Angaben zur Veröffentlichung / Publication details:

Eremina, R. M., Mikhail V. Eremin, V. N. Glazkov, Hans-Albrecht Krug von Nidda, and Alois Loidl. 2003. "Anistropic exchange interactions in CuGeO3 probed by electron spin resonance spectroscopy." *Physical Review B* 68 (1): 014417. https://doi.org/10.1103/PhysRevB.68.014417.

Anisotropic exchange interactions in $CuGeO_3$ probed by electron spin resonance spectroscopy

R. M. Eremina,[1,4] M. V. Eremin,[2,4] V. N. Glazkov,[3,4] H.-A. Krug von Nidda,[4,*] and A. Loidl[4]
[1]*E. K. Zavoisky Physical Technical Institute, 420029 Kazan, Russia*
[2]*Kazan State University, 420008 Kazan, Russia*
[3]*P. L. Kapitza Institute for Physical Problems, 117334 Moscow, Russia*
[4]*Experimentalphysik V, Elektronische Korrelationen und Magnetismus, Institut für Physik, Universität Augsburg, 86135 Augsburg, Germany*
(Received 20 February 2003; published 15 July 2003)

The analysis of the anisotropy of the electron-spin resonance (ESR) linewidth in $CuGeO_3$ taken at different temperatures, allows one to obtain relations between the anisotropic exchange-interaction parameters. The anisotropy of the ESR linewidth can be understood purely in terms of the symmetric anisotropic exchange interaction. The intrinsic anisotropic exchange parameters of the copper spins are determined for intrachain and interchain interactions and their microscopic origin is explained. All conclusions about the nature of the anisotropy are in agreement with the reported crystal structure for $CuGeO_3$. The temperature dependence of the anisotropic exchange parameters can be related to the lattice fluctuations as detected by other experimental techniques. An empirical formula for the temperature dependence of the ESR linewidth is suggested.

DOI: 10.1103/PhysRevB.68.014417 PACS number(s): 75.30.Et, 76.20.+q, 76.30.Fc, 73.90.+f

I. INTRODUCTION

Low-dimensional magnets are a subject of intense interest due to the fact that quantum phenomena play an important role in these compounds. For example, several organic quasi-one-dimensional spin $S=1/2$ Heisenberg antiferromagnets do not show three-dimensional magnetic order, but exhibit a spin-Peierls transition into a singlet $S=0$ ground state characterized by the dimerization of neighboring spins. The quasi-one-dimensional $S=1/2$ antiferromagnet $CuGeO_3$ is the only inorganic compound demonstrating a spin-Peierls transition up to now, with a transition temperature $T_{SP} \approx 14$ K.[1] Therefore this system has attracted considerable attention during the last decade.[2]

The crystal structure of $CuGeO_3$ is well determined.[3,4] At high temperatures the unit cell contains two formula units [space group *Pbmm* (D_{2h}^5)]. Each copper ion (Cu^{2+}, spin $S=1/2$) is surrounded by six oxygen ions forming a slightly deformed octahedron.[4] Chains of edge-sharing CuO_6 octahedra aligned along the c axis determine the quasi-one-dimensional magnetic properties of $CuGeO_3$. The two oxygen octahedra within the unit cell share the apical oxygen. Hence, there are two inequivalent chains which differ by the orientation of the octahedron axis in the ab plane. At the spin-Peierls transition a dimerization of the chains occurs, accompanied by the alternation of the intrachain exchange integral, and an energy gap opens between the singlet ground state and triplet excited states. Due to the three dimensionality of the crystal lattice, the dimerization of the chain is accompanied by a doubling of the lattice periodicity along the a and c axes and a small tilting of the oxygen octahedra.[4] After reexamination of the crystal structure by Hidaka *et al.*,[5] the existence of small modulations of the crystal structure was suggested. These modulations lead to a lowering of the symmetry already in the high-temperature phase yielding the space group $P2_12_12$ (D_2^3) and to an increase of the unit cell (fourfold along the c direction, and twofold along a).

By now, the values of the isotropic Heisenberg-exchange integrals are well established from susceptibility measurements and neutron-scattering experiments:[4,6,7] the intrachain exchange constants for the nearest and next-nearest neighbors are $J_c=10.4$ meV and $J_c^{nnn}=3.28$ meV, respectively; the interchain coupling parameters along the a and b axes are smaller, with $J_a/J_c=-0.011$ and $J_b/J_c=0.11$. The exchange-integral values of the possible anisotropic exchange interactions are still not known. Furthermore, the nature of the anisotropic exchange interaction in $CuGeO_3$ is still a subject of discussion. Electron-spin resonance (ESR) is a convenient method to probe anisotropic spin-spin interactions. The ESR linewidth reflects the average amplitude of the fluctuating field on the magnetic-ion site, which can be directly connected to the parameters of the anisotropic spin-spin interactions.

The ESR signal of $CuGeO_3$ consists of a single exchange-narrowed resonance line[8–10] with nearly temperature independent g tensors $g_a=2.16$, $g_b=2.26$, and $g_c=2.07$, except for the lowest temperatures ($T<5$ K), where a splitting of the ESR line occurs due to the formation of clusters and domain walls.[11] Near the spin-Peierls transition the ESR linewidth exhibits its minimum value of about 30 Oe and diverges to lower temperatures in the spin-Peierls phase, until the line splitting appears. Above the spin-Peierls transition the linewidth increases monotonically with increasing temperature, reaching values of about 1 kOe at room temperature and approaching saturation above 800 K.[12] In addition, the linewidth shows a pronounced anisotropy with the largest values for the magnetic field applied along the b axis. The increase of the linewidth with increasing temperature was found to be in qualitative agreement with the product of temperature and susceptibility ($\Delta H \propto T\chi$), as predicted for one-dimensional antiferromagnetic chains due to the contribution of long-wavelength spin-fluctuation modes.[8] However, the underlying interaction of the line broadening is still under debate.

Yamada *et al.*[12] have suggested that the temperature de-

pendence of the ESR linewidth should be ascribed to the Dzyaloshinsky-Moriya (DM) interaction (i.e., antisymmetric anisotropic exchange interaction). However, this suggestion contradicts to the crystal structure determined by Braden *et al.*,[4] since it contains an inversion center between neighboring Cu ions. The refinement of the crystallographic structure by Hidaka *et al.*[5] could not solve this problem. Although it was argued that the larger unit cell of the refined structure does not exhibit an inversion center along the c axis any more, and therefore allows for the DM interaction to exist, again the local symmetry cancels the intrachain DM interaction due to the equivalence of the two Cu-O-Cu exchange bridges, which connect two neighboring Cu ions in the chain.

Pilawa[13] argued that the anisotropy of the ESR linewidth in $CuGeO_3$ should be attributed to the symmetric anisotropic exchange interaction. This allows one to obtain a good description of the orientation dependence of the linewidth. However, two open questions remain in that approach. First, the experimentally observed high-temperature linewidth strongly exceeds conventional estimates of the contribution due to symmetric anisotropic exchange. Second, it was necessary to use the orientation of the anisotropic exchange tensor as a fitting parameter, while it has to be rigidly defined by the orientation of the CuO_6 octahedra. Nevertheless, recent field-theory calculations by Oshikawa and Affleck show that the observed temperature dependence of the ESR linewidth can be qualitatively explained in terms of the symmetric anisotropic exchange.[14]

Here we present a detailed reinvestigation of the angular and temperature dependence of the ESR linewidth in $CuGeO_3$. Based on our recent results in the related antiferromagnetic chain compound $LiCuVO_4$,[15] the large absolute value of the linewidth measured at high temperatures can be explained from the specific geometric situation of the ring exchange in the chains of edge-sharing CuO_6 octahedra. We will show that the anisotropy of the linewidth can be well described by symmetric anisotropic exchange interactions, where not only the intrachain but also the interchain contributions have to be taken into account. Then it is possible to keep the orientation of the anisotropic exchange tensor fixed in agreement with the crystal structure. The extracted exchange parameters and their temperature dependences reflect the peculiarities reported from neutron scattering, electron diffraction and ultrasonic absorption.

II. THEORETICAL BACKGROUND

A. General remarks

The theory of the ESR linewidth is well-developed for conventional three-dimensional (3D) exchange-coupled spin systems.[16,17] It has been shown that in the case of sufficiently strong exchange interaction the ESR spectrum is narrowed into a single Lorentz line with a linewidth ΔH (half width at half maximum) determined by the second moment M_2 due to anisotropic interactions and the exchange frequency ω_{ex} caused by the isotropic Heisenberg exchange $\mathcal{H}_{ex}^{ij}=J\mathbf{S}_i\mathbf{S}_j$ between neighboring spins $\mathbf{S}_i$ and $\mathbf{S}_j$ as[16]

$$\Delta H=\frac{\hbar}{g\mu_B}\frac{M_2}{\omega_{ex}}. \tag{1}$$

Here g denotes the g value, $\hbar$ the Planck constant, and μ_B the Bohr magneton. At high temperatures ($T\to\infty$) both the second moment M_2 and the exchange frequency ω_{ex} are temperature independent and can be expressed via microscopic Hamiltonian parameters. The second moment shows an orientation dependence with respect to the external magnetic field, which is characteristic for the anisotropic interaction responsible for the line broadening. The exchange frequency approaches the isotropic value $\hbar\omega_{ex}\approx J$.

Due to the fact that these results are obtained in the high-temperature approximation, when all states are equally populated, additional considerations are necessary concerning the temperature regime, where this approximation fails. In strongly exchange-coupled systems this approximation is only valid at temperatures exceeding the exchange-integral value J. For 3D magnets this restriction is not very severe, because at temperatures $k_BT\sim J$ long-range order is established (k_B denotes the Boltzmann constant). However, in 1D magnets long-range order, if it exists, is established only due to the weak interchain interactions at $k_BT\ll J$. Thus, there is a wide temperature range in the paramagnetic state where antiferromagnetic correlations have to be taken into account.

An expansion of the ESR linewidth theory to the case of low-dimensional systems at temperatures $k_BT<J$ was performed, e.g., by Soos,[18] who included the temperature dependence of the spin-correlation functions within the traditional formalism. Recently, Oshikawa and Affleck[14] used field-theory methods to derive the temperature dependence of the ESR linewidth deeply in the one-dimensional regime ($k_BT\ll J$). One relevant result of these papers is that, if the ESR linewidth is due to a single anisotropic interaction, then the temperature dependence of the linewidth is an isotropic function. This means that for all temperatures the relative anisotropy of the ESR linewidth ΔH should be the same as in the high-temperature approximation $T\to\infty$, i.e.,

$$\Delta H(T,\theta,\phi)=F(T)\Delta H(\theta,\phi)|_{T\to\infty}. \tag{2}$$

The orientation of the external magnetic field $\mathbf{H}$ is determined by polar and azimuth angle θ and ϕ. The isotropic function $F(T)$ approaches unity at high temperatures $T\gg J/k_B$.

The behavior of the function $F(T)$ at finite temperatures depends on the origin of the anisotropic interaction which causes the line broadening. For the case of symmetric anisotropic exchange interaction, $F(T)$ was predicted to increase linearly with increasing temperature at $k_BT\ll J$, while for the antisymmetric DM exchange interaction a divergence $\propto 1/T^2$ is expected at low temperatures.[14] The exact temperature dependence of $F(T)$ is unknown. However, Eqs. (1) and (2) allow us to write down a simple expression for the normalized linewidth:

$$\frac{\Delta H(T,\theta,\phi)}{\Delta H(T,\mathbf{H}\|\mathbf{l})}=\frac{\Delta H(\theta,\phi)|_{T\to\infty}}{\Delta H(\mathbf{H}\|\mathbf{l})|_{T\to\infty}}=\frac{M_2(\theta,\phi)|_{T\to\infty}}{M_2(\mathbf{H}\|\mathbf{l})|_{T\to\infty}}. \tag{3}$$

Here **l** is some fixed direction. As it follows from Eq. (3), the normalized linewidth should be temperature independent as long as only one type of interaction is responsible for it. It is also free from the uncertainty in the definition of the exchange frequency ω_{ex}. The price of this simplicity is that we can obtain only ratios of microscopic Hamiltonian parameters, once we express second moments in Eq. (3).

Based on these findings we turn to the special case of $CuGeO_3$, now. To describe the anisotropy of the linewidth the contributions of the two inequivalent chains have to be coupled accurately. For a single chain the ESR linewidth is determined by[16]

$$\Delta H_{1,2}=\frac{\hbar}{g\mu_B}\frac{(M_2^{(1,2)}+M_2^{\perp})}{\omega_{ex}}. \tag{4}$$

Here $M_2^{(1,2)}$ are the second moments calculated for each of the two inequivalent chains, caused by the anisotropic exchange between the copper spins within one chain, $M_2^{\perp}$ is the contribution due to the interchain interaction. Details of the calculation of the second moments are given in the Appendix. The exchange frequency $\omega_{ex}\approx J_c/\hbar$ is expressed via the superexchange parameter $J_c=10.4$ meV between nearest-neighbor copper spins in the chain. Because the orientations of the CuO_6 octahedra of neighboring chains are different with respect to the external magnetic field, we have to take into account two different resonance fields H_1 and H_2 and linewidths ΔH_1 and ΔH_2 of the respective chains for a given field orientation. Let us introduce $\delta=H_1-H_2$ and $g\mu_B\Omega=J_{12}$, where J_{12} denotes the interchain exchange-coupling constant and Ω the respective exchange field. Applying the theory of adiabatic transformation of magnetic-resonance spectra,[19] one can deduce that for $\Omega>\delta$ the resulting ESR spectrum will be one Lorentz line with the center field $H_{res}=(H_1+H_2)/2$, and a linewidth

$$\Delta H=\frac{\frac{\Delta H_1+\Delta H_2}{2}+\frac{2\delta^2}{\Omega}+\frac{(\Delta H_1+\Delta H_2)^2}{8\Omega}}{1+\frac{\Delta H_1+\Delta H_2}{2\Omega}}. \tag{5}$$

In first respect, the linewidth of the two inequivalent chains results from a simple averaging procedure. The additional contribution to the line broadening $2\delta^2/\Omega$ is reminiscent to the well known expression for the linewidth, caused by the difference of the g factors of interacting magnetic centers.[20]

B. Anisotropic interactions in $CuGeO_3$

To discuss the anisotropic exchange interactions in $CuGeO_3$, we return to the crystallographic structure which is basically formed by two inequivalent chains of edge-sharing CuO_6 octahedra running along the c direction (see Fig. 1). The intrachain exchange interactions are realized via Cu-O2-Cu superexchange paths, the interchain interactions are transferred via the apical oxygen O1. Note that the Cu-O2-Cu angle is close to 90° (see Ref. 4); thus the contribution of this path to the Heisenberg exchange-integral value is very small or even ferromagnetic and the enhancement of the superexchange due to the side-group effects (Ge) has to be taken into account.[21,22] However, the anisotropic exchange interaction is realized via excited electron orbitals, mixed with the ground state by the spin-orbital interaction. Therefore, this "90°" argument is not applicable to the calculation of the anisotropic interaction constants, and the Cu-O2-Cu superexchange path will govern the values of the intrachain anisotropic exchange constants.

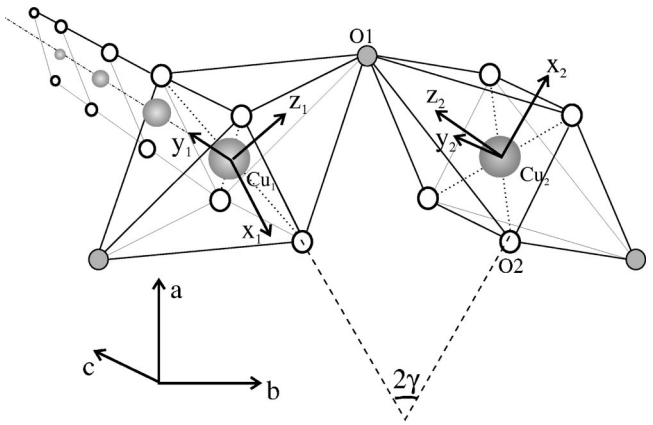

FIG. 1. Detail of the $CuGeO_3$ structure: Orientation of the local coordinate systems (x_1,y_1,z_1) and (x_2,y_2,z_2) for the inequivalent chains with angle $\gamma\approx 34°$ (see Ref. 4). The positions of the Ge ions are not shown.

Since the anisotropic exchange interaction is realized via Cu-O2-Cu superexchange paths, its symmetry is bound to the copper-oxygen ribbons, and the anisotropic exchange-interaction tensor should be diagonal in the local coordinates with the y axis along the chain direction and the z axis perpendicular to the ribbon plane (see Fig. 1). Hence, the symmetric intrachain anisotropic exchange interaction between two neighboring spins $\mathbf{S}_i$ and $\mathbf{S}_j$ can be written in local coordinates as

$$\mathcal{H}_{intra}^{(i,j)}=J_{xx}S_i^xS_j^x+J_{yy}S_i^yS_j^y+J_{zz}S_i^zS_j^z, \tag{6}$$

where $J_{xx}+J_{yy}+J_{zz}=0$. The local coordinates for inequivalent chains are different. Note that the z-axis is not parallel to the Cu-O1 bonds. The 90° geometry and quantum interference between different exchange paths (so called ring-exchange) in the Cu-O2 ribbon strongly enhance the values of the anisotropic exchange constants. These values remain stable on slight deviations from the exact 90° bond angle, whereas the isotropic exchange constant J is reduced and even crosses zero by small changes of the bond geometry.[23] This explains the difficulty to estimate the anisotropic exchange constants (J_{AE}) from g-shift and isotropic exchange, because here the isotropic exchange constant $J\equiv J_{xy,xy}$ between the d_{xy} ground states of two neighboring copper ions is not comparable to the isotropic exchange J_{xy,x^2-y^2} between the d_{xy} ground state and the neighboring $d_{x^2-y^2}$ excited state, which is necessary for the estimation[24] $J_{AE}\sim[(g-2)/g]^2J_{xy,x^2-y^2}$. Calculations for the geometrically similar compound $LiCuVO_4$ predict a value of the anisotropic exchange constant $J_{zz}/k_B\approx -1.8$ K in good agreement with the experimental values $J_{zz}/k_B=-1.75$ K,

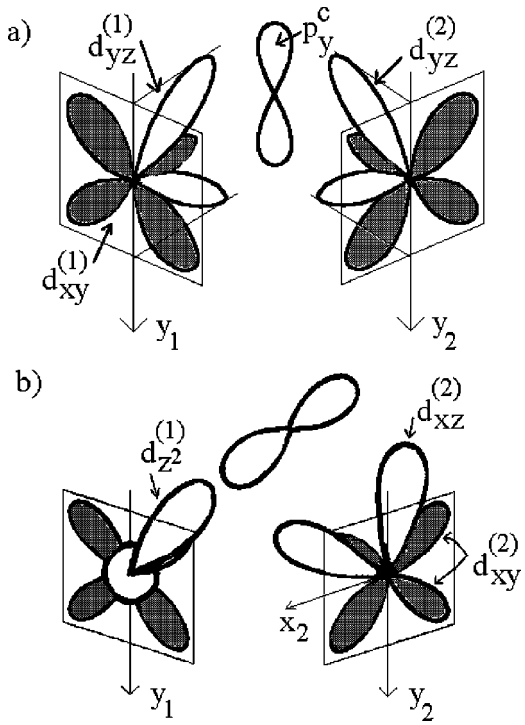

FIG. 2. Schematic pathway of anisotropic spin-spin coupling between copper d_{xy} states via (a) filled d_{yz} and oxygen p_y^c states—the d_{xy} and d_{yz} states are coupled via intra-atomic Coulomb interaction as well as due to spin-orbit coupling, (b) occupied d_{z^2},$d_{xz}^{(2)}$ and p-oxygen states—d_{z^2} and $d_{xy}^{(1)}$ are coupled via intra-atomic Coulomb repulsion, whereas $d_{xy}^{(2)}$ and $d_{xz}^{(2)}$ are coupled due to spin-orbit coupling.

$J_{xx}/k_B=0.16$ K and $J_{yy}/k_B=-0.02$ K.[15] Using the above normalization, this yields $J_{xx}/k_B=0.70$ K, $J_{yy}/k_B=0.52$ K, $J_{zz}/k_B=-1.22$ K. At the same time, the intrachain DM interaction vanishes due to the symmetric bond geometry.

For the interchain interaction, the analysis of the relevant orbitals (see Sec. II C) shows that it will have a dominating component along the chain direction, i.e., along the c axis. Thus, for two nearest spins located in neighboring chains 1 and 2, it is given by

$$\mathcal{H}_{inter}=A_{cc}S_c^{(1)}S_c^{(2)}, \tag{7}$$

where $S_c^{(1,2)}$ are spin projections on the chain direction. In principal the interchain bond geometry via the apical oxygen allows the existence of the DM interaction. However, as there is no divergence $\Delta H\propto 1/T^2$ observed in the experiment for $T>T_{SP}$, the DM interaction seems to be of minor importance.

C. Microscopic estimation of the anisotropic exchange between different chains

Before we will describe the experimental results, we want to show that the expected contribution of the anisotropic interchain exchange A_{cc} is Ising-like and of comparable order of magnitude as the intrachain contribution. According to the microscopic theory, the anisotropic symmetric exchange-interaction parameters can be calculated as a combination of isotropic superexchange via excited states and spin-orbit coupling of those excited states with the ground state (for a short review, see Ref. 25). The schematic pathways of the possible spin-spin coupling between two neighboring chains are presented in Fig. 2. The hole of the $3d^9$ electron configuration of Cu^{2+} is located in the ground state d_{xy}. In the upper picture (a) the excited d_{yz} states of both copper ions couple via the bridge-oxygen p_y orbital, in the lower picture (b) the excited d_{z^2} state of one copper ion is coupled to the excited d_{xz} state of the other copper ion via a linear combination of the bridge-oxygen p_x and p_z orbitals. To determine the relevant components of the anisotropic exchange tensor, we have to consider the matrix elements of the spin-orbit coupling $\xi\mathbf{L}\cdot\mathbf{S}$ between the ground state and excited states of the copper ion. In case (a) the matrix elements $\langle xy|L_x|yz\rangle=\langle xy|L_z|yz\rangle=0$ vanish and only the L_y component of the orbital momentum $\mathbf{L}$ yields a nonzero exchange parameter A_{yy} and spin projection S_y. In case (b) the only parameter which does not vanish is the parameter A_{xx} from the spin-orbit coupling of the ground state with the d_{xz} orbital. The states d_{z^2} and d_{xy} are not coupled via spin-orbit interaction but via intra-atomic Coulomb repulsion.

Following this scheme, we obtain for the interchain anisotropic exchange parameters

$$A_{yy}=-\left(\frac{\lambda}{\Delta_{xy,yz}}\right)^2\frac{t_\pi^2}{\Delta_{12}^2}2(3B+C)\frac{t_\pi^2}{\Delta_\pi^2},$$

$$A_{xx}=-\left(\frac{\lambda}{\Delta_{xy,xz}}\right)^2\frac{t_\pi^2}{\Delta_{12}^2}2(4B+C)\frac{t_\sigma^2}{\Delta_\pi^2}\sin^2(2\gamma), \tag{8}$$

where the first expression corresponds to Fig. 2(a) and the second one is illustrated in Fig. 2(b). Here λ is the spin-orbit coupling and $\Delta_{xy,yz}\approx\Delta_{xy,xz}$ the crystal-field splitting between the respective d states of Cu^{2+}. For σ and π bonds between copper and oxygen, t_σ and t_π denote the transfer integrals and Δ_π and Δ_σ the charge-transfer energy. Δ_{12} is the charge-transfer energy from one Cu site to the other Cu site. The parameters $B\approx 955$ cm^{-1} and $C\approx 4234$ cm^{-1} denote the Racah parameters of the Coulomb interaction between the copper electrons.[26] After transformation into crystallographic coordinates (cf. the Appendix), the anisotropic exchange parameters read $A_{cc}=A_{yy}$, $A_{aa}=A_{xx}\cos^2\gamma$, and $A_{bb}=A_{xx}\sin^2\gamma$. After renormalization $A'_{cc}=A_{yy}-A_{xx}/2$ the two other parameters $|A'_{aa}|,|A'_{bb}|\ll|A'_{cc}|$ can be approximately neglected and we obtain Eq. (7).

The ratio between the spin-orbit coupling parameter λ and the energy of the crystal-field splitting $\Delta_{xy,xz}$ between the states d_{xy} and d_{xz} is approximately given by $(\lambda/\Delta_{xy,xz})^2\approx(g_\perp-2)^2\approx 0.01$. The ratio of the oxygen-copper transfer parameters t_σ and t_π to the charge transfer energy $\Delta_\pi\approx\Delta_\sigma$ is known for oxides from studies of the transferred hyperfine interactions as $t_\pi^2/\Delta_\pi^2\approx t_\sigma^2/\Delta_\pi^2\approx 0.077$.[27] The oxygen-copper transfer integrals are approximately equal ($t_\pi\approx t_\sigma$), and according to different estimations their value is about $t_\sigma\simeq 1.3$–2.5 eV.[28,29] The charge-transfer

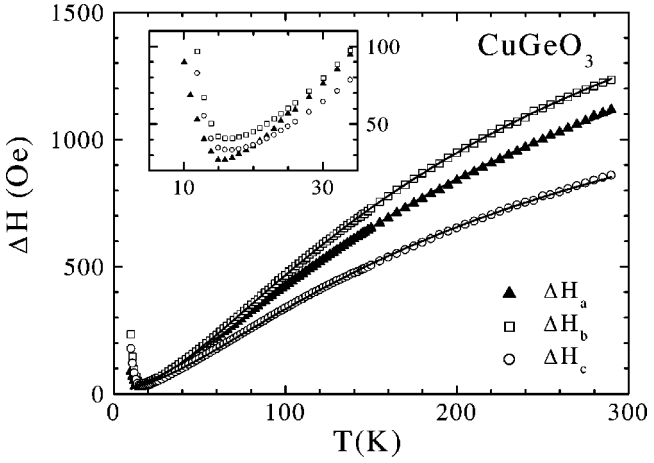

FIG. 3. Temperature dependence of the ESR linewidth in $CuGeO_3$ measured at the microwave frequency $\nu = 9.48$ GHz for the magnetic field applied parallel to the three crystallographic axes. The fit curves were obtained using Eq. (9). The respective parameters are collected in Table I. Inset: linewidth in the low-temperature regime near T_{SP}.

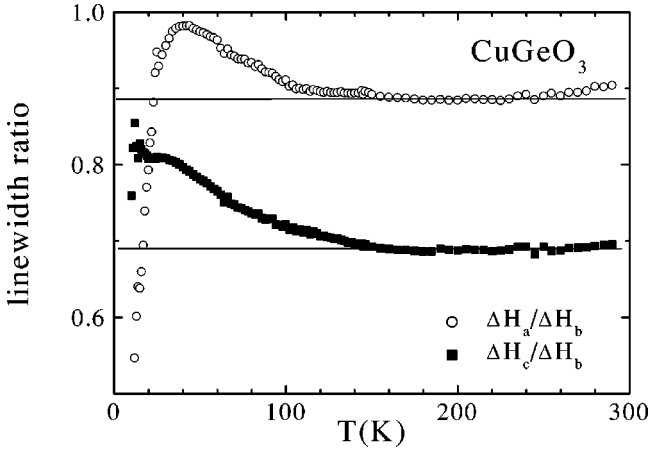

FIG. 4. Temperature dependence of the linewidth ratios $\Delta H_a/\Delta H_b$ and $\Delta H_c/\Delta H_b$ in $CuGeO_3$ determined with respect to the maximum linewidth at $H \| b$.

energy between the Cu ions is about $\Delta_{12} \simeq 6$ eV.[28] Therefore we can use $(t_\pi/\Delta_{12})^2 \approx 0.1$. Substituting the structural angle $2\gamma = 68°$ between the chains, we get $A_{cc}/k_B \approx -0.7$ K, which shows that the interchain exchange coupling cannot be neglected compared with the intrachain exchange.

III. EXPERIMENTAL DETAILS

Single crystals of $CuGeO_3$ were grown from the high-purity components by means of spontaneous crystallization from the flux melt at slow cooling. They are the same as the main set of samples investigated in Ref. 11. The concentration of the impurities Fe, Ni, Mn, and Co does not exceed 10^{-4} per Cu ion. The 20-fold decrease of the susceptibility below the spin-Peierls transition temperature indicates the absence of structural defects, as well.[11] For the ESR measurements we have used single crystals with a typical size of $0.5 \times 2 \times 4$ mm^3.

The ESR measurements were performed in a Bruker ELEXSYS E500 CW spectrometer at *X*-band frequency (9.5 GHz), equipped with a continuous gas-flow cryostat for He (Oxford Instruments). The ESR spectra record the power P_{abs} absorbed by the sample from the transverse magnetic microwave field as a function of the static magnetic field H. The signal-to-noise ratio of the spectra is improved by detecting the derivative $\partial P_{abs}/\partial H$ with the standard field-modulation technique. The $CuGeO_3$ single crystals were glued on a suprasil-quartz rod, which allowed the rotation of the sample around defined crystallographic axes.

The observed ESR absorption is well described by a single Lorentz line except for the lowest temperatures ($T < 5$ K) where the above mentioned splitting of the ESR line occurs.[11] The resonance field H_{res} and linewidth ΔH have been determined by numerical fitting as described, e.g., in Ref. 15.

IV. EXPERIMENTAL RESULTS AND DISCUSSION

A. Temperature dependence of the ESR linewidth

Figure 3 presents the detailed temperature dependence of the ESR linewidth at $T < 300$ K for the static magnetic field applied along the three crystallographic axes. For all three orientations the linewidth increases monotonically above the spin-Peierls transition, first with a slightly positive curvature, which changes into a negative curvature above 100 K indicating the saturation behavior observed by Yamada *et al.*[12] at $T > 700$ K. The maximum linewidth is always observed for $H \| b$. At high temperatures the linewidth for $H \| a$ is about 10% smaller compared to the width for $H \| b$, while that for $H \| c$ is about 30% smaller. With decreasing temperature this anisotropy changes: near $T \approx 22$ K the linewidths for $H \| a$ and $H \| c$ are equal, and as the temperature decreases further, the linewidth remains smallest at $H \| a$ (see the inset in Fig. 3). The minimum of the linewidth is observed slightly above the spin-Peierls transition $T_{SP} \approx 14$ K. On crossing the spin-Peierls temperature the linewidth starts to increase for all orientations. This increase is due to the freezing out of the triplet excitations, which gradually weakens the exchange narrowing. It is interesting to note that the splitting of the main ESR line observed at low temperatures ($T < 5$ K) (Ref. 11) is broadest for $H \| b$ and smallest for $H \| a$, i.e. exactly as the linewidth anisotropy below 22 K.

Returning to the temperature regime above the spin-Peierls transition, it is instructive to plot the linewidth ratios $\Delta H_a/\Delta H_b$ and $\Delta H_c/\Delta H_b$ with respect to the maximum linewidth (Fig. 4). Starting at room temperature, both ratios remain constant at 0.9 and 0.7, respectively, down to 120 K. On further decreasing the temperature, their values continuously increase by 0.1. Below 40 K the ratio $\Delta H_c/\Delta H_b$ saturates at 0.8, whereas $\Delta H_a/\Delta H_b$ reaches its maximum near 40 K and then strongly decreases, indicating the crossing point of ΔH_a with ΔH_c at 22 K.

As it was discussed above from Eq. (3), if the linewidth is determined by only one interaction—in our case the symmetric anisotropic exchange interaction—then the normalized linewidth should be temperature independent. For $120 \leqslant T$

TABLE I. Parameters determined from fits on the temperature dependence of the linewidth using Eq. (9).

	$\Delta H(\infty)$ (Oe)	$2C_1$ (K)	C_2 (K)
$H\|a$	2269±30	239±5	42±2
$H\|b$	2502	229	36
$H\|c$	1726	235	42

$\leqslant$300 K this condition is clearly fulfilled and even holds true up to 800 K, as Yamada *et al.* have already proven experimentally.[12] The deviations observed below 120 K may arise on different grounds. One reason can be that another interaction becomes important at low temperatures: e.g., the interchain Dzyaloshinsky-Moriya interaction may give rise to a divergent contribution of the interchain interaction at low temperatures, or the soliton dynamics can influence the spin-spin relaxation, or simply some contribution due to impurities may affect the linewidth. But the observed deviations may also result from a change of the exchange integrals due to lattice fluctuations on approaching the spin-Peierls transition. This last possibility is supported by several independent experiments:

By inelastic neutron scattering Braden *et al.* identified two low-lying phonon modes associated with the structural distortion in the dimerized phase[30] and studied their temperature dependence. The eigenfrequencies of these modes remain approximately constant down to 150 K at 3.1 and 6.5 THz. On further cooling they exhibit an increasing shift to higher frequencies and a pronounced line broadening already far above the spin-Peierls transition. The frequency shift saturates below 30 K at values about 10% higher compared to room temperature. In electron-diffraction experiments Chen and Cheong detected a diffuse scattering with the shape of an infinite ribbon parallel to the chain direction also clearly above the spin-Peierls transition.[31] Its intensity rises rapidly below 100 K and again saturates below 30 K. The authors propose that the diffuse scattering is caused by low-frequency twisting vibrations of the Cu-O2 ribbons along the chains. In addition Raman-scattering experiments revealed an anomaly with a quite similar behavior. Another important observation, which is worth mentioning in this context, is reported from ultrasonic experiments: Quirion *et al.* found a broad anomaly in the temperature dependence of the sound velocity along the *c* axis centered around 100 K.[32] This anomaly is attributed to magnetoelastic couplings.

All these experiments reveal a systematic change of the lattice couplings below 150 K, which should affect the anisotropic exchange as well and therefore justifies an evaluation of the resonance linewidth in terms of symmetric anisotropic exchange only. This is in agreement with the monotonic increase of the linewidth with increasing temperature above T_{SP}, approaching saturation for $T\rightarrow\infty$. The deviation from a purely linear behavior at $T\ll J/k_B$ is not in contradiction to Oshikawa and Affleck, because their theory for ideal 1D systems does not take into account structural fluctuations, which exist already above the spin-Peierls transition, and therefore holds only in the case $T\gg T_{SP}$.[14]

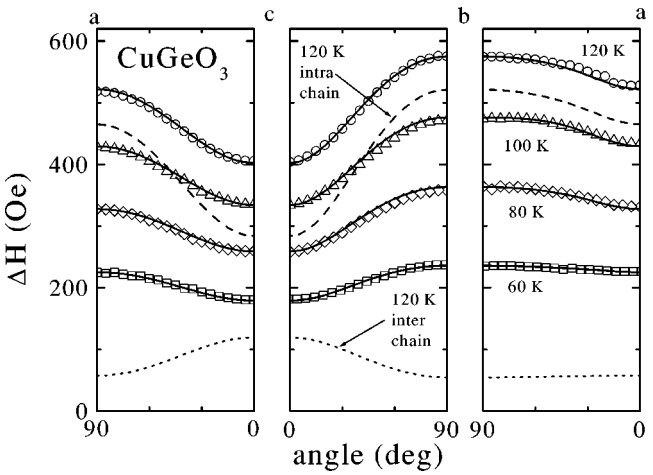

FIG. 5. Angular dependence of the resonance linewidth for the magnetic field rotated within the three crystallographic planes at different temperatures between 60 and 120 K. Solid lines: fit curves obtained by Eq. (5). For $T=120$ K the contributions of intrachain and interchain exchange are indicated by dashed and dotted lines, respectively.

For a quantitative description of the temperature dependent isotropic function $F(T)$ in Eq. (2), we tried to empirically approximate the linewidth at $T>T_{SP}$ by

$$\Delta H(T)=\Delta H(\infty)\exp\left(-\frac{2C_1}{T+C_2}\right), \tag{9}$$

where $\Delta H(\infty)$, C_1, and C_2 are treated as fitting parameters. The data were evaluated independently for the three orientations. Equation (9) nicely fits the temperature dependence of the linewidth above the spin-Peierls transition, as shown in Fig. 3. The results are given in Table I. The asymptotic values $\Delta H(\infty)$ yield the same linewidth ratios as observed above 120 K. The parameters C_1 and C_2 are approximately the same for all three curves, where the smaller C_2 in ΔH_b accounts for the changes of the linewidth ratios observed below 120 K. The extrapolation of the linewidth data with these parameters to 800 K is found to be about 10% smaller than Yamada's experimental data,[12] which is still a good agreement taking into account the large temperature difference between 300 and 800 K. Note that the parameter C_1 corresponds to the isotropic exchange constant *J*. This is reasonable, because the parameter C_1 indicates the transition from the strongly correlated one-dimensional regime at low temperatures $T\ll J/k_B$ to the purely paramagnetic regime $T\gg J/k_B$, where the high-temperature approximation is valid. The parameter C_2 is comparable to $\sqrt{J_bJ_c}=3.4$ meV, which gives an estimate for the hypothetical Néel temperature, and therefore C_2 seems to be connected with the interchain coupling. A relation of C_2 to the dimerization may also be discussed, as the singlet-triplet gap of the spin-Peierls phase is of similar magnitude. But we would like to recall that Eq. (9) has been found empirically and has no underlying microscopic picture.

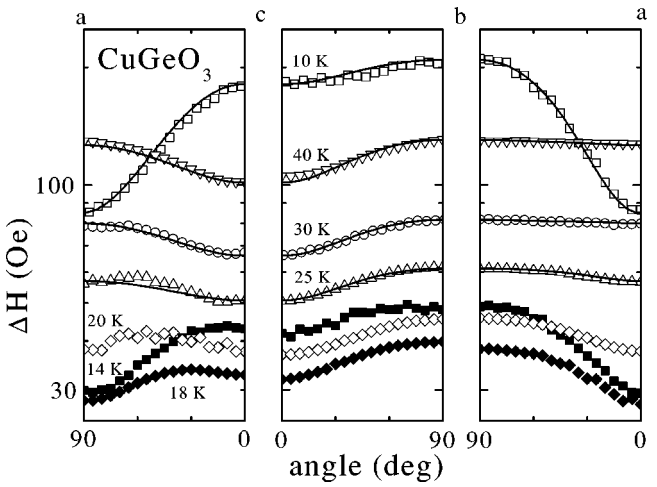

FIG. 6. Angular dependence of the resonance linewidth for the magnetic field rotated within the three crystallographic planes at different temperatures between 10 and 40 K. The logarithmic scale of the ordinate emphasizes the changes in the data between 14 and 25 K. Solid lines: fit curves obtained by Eq. (5).

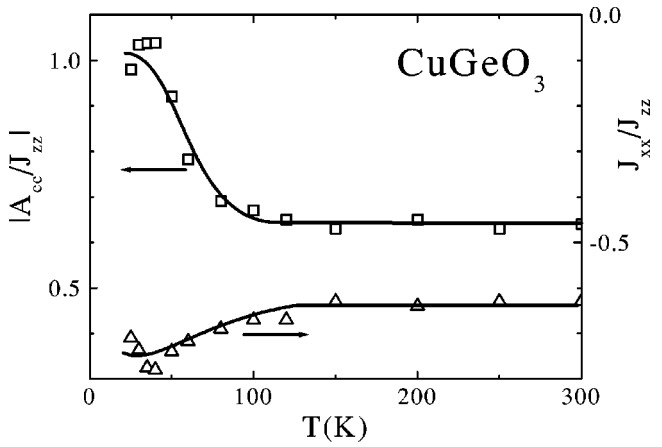

FIG. 7. Temperature dependence of the normalized anisotropic exchange parameters $|A_{cc}/J_{zz}|$ (squares) and J_{xx}/J_{zz} (triangles).

B. Determination of the exchange parameters from the angular dependence

Now, we focus our attention on the angular dependence of the ESR linewidth, which we investigated in detail for the three crystallographic planes at several temperatures between 10 K and room temperature. Typical data are shown in Figs. 5 and 6 for selected temperatures. Considering the relative linewidth normalized to the value for $H||b$, the angular dependence at $T=120$ K coincides well with the data measured at higher temperatures, as one expects from the linewidth ratios in Fig. 4. To lower temperatures the relative amplitudes change but the general features are still maintained down to about 25 K. Finally, below 25 K also the general pattern of the angular dependence changes and the linewidth ΔH_a becomes smallest instead of ΔH_c.

The angular dependence of the ESR linewidth was approximated by Eqs. (4) and (5), is illustrated in Figs. 5 and 6. Like in the case of $LiCuVO_4$, each chain gives the maximum contribution to the linewidth for the magnetic field applied perpendicular to the plane with the ring-exchange geometry (i.e., the Cu-O2 ribbons). Averaging of the contributions from the two inequivalent chains in $CuGeO_3$ results in a large linewidth for the field applied perpendicular to the chain direction with a weak variation in the *ab* plane. However, with the fixed orientation of the anisotropic exchange tensor, it was not possible to describe the data by the intrachain contribution (dashed lines for 120 K) alone. An accurate fit of the *ab* plane by the intrachain contribution, only, results in too small a linewidth in the *c* direction. This problem is solved by the additional interchain contribution (dotted lines), which increases the linewidth in the *c* direction with respect to the *ab* plane, and yields a satisfactory description of the data.

For all temperatures under investigation the results of the fit procedure are plotted in Fig. 7. Only the relative exchange parameters J_{xx}/J_{zz} and $|A_{cc}/J_{zz}|$ are shown. The spectral functions f_i (cf. the Appendix) were kept fixed at all temperatures, for the interchain contribution exactly at 1 and for the intrachain contribution $f_1/f_3=0.95$ and $f_2/f_3=1.05$ was chosen. Similar to the case of $LiCuVO_4$ this was necessary to improve the fit for intermediate angles. The observation that all spectral functions are near unity is in agreement with the fact that the exchange interaction J is by far larger than the Zeeman splitting. In this case secular and nonsecular parts of the second moment should fully contribute to the linewidth.[16]

Below 25 K an unequivocal description of the angular dependences within the framework of our model was not possible. As one can see in Fig. 6, there is the crossing of the linewidths ΔH_a and ΔH_c at 21 K, which is accompanied by an additional modulation $\propto\cos 4\theta$ of the linewidth in the *ac* plane. In principal, this can be described by our equations, if we allow for strong changes of the spectral functions f_i in the interchain contribution. However, the influence of additional anisotropic interactions cannot be excluded here. At temperatures below the spin-Peierls transition these modulations again disappear, but the general features of the anisotropy developed at 21 K are preserved with the minimum of the linewidth for the magnetic field applied in the *a* direction. A good fit of the data at 10 K can be achieved with the interchain contribution, only, with $A_{cc}/A_{bb}=-0.78$ and $A_{aa}/A_{bb}=-0.22$ (using the normalization $A_{aa}+A_{bb}+A_{cc}=0$). However, a dominant tensor component A_{bb} is not expected from our estimations at all. Probably, at these temperatures the description of the linewidth in terms of anisotropic exchange is not applicable any more, because already slightly below T_{SP} the signal of the triplet excitations is mixed with contributions from the multi-spin objects, which govern the complicated spectrum at lower temperatures after freezing out of the triplet excitations.[11] Some of these objects possess a spin $S>1/2$, which is sensitive to the crystal field. The angular dependence of the linewidth at 10 K follows the splitting at 4 K. Therefore, it seems likely that the influence of the crystal field has also to be taken into account for the description of the anisotropy and already gains partial influence in the transition regime $T\approx T_{SP}$.

Due to these difficulties we confined the presentation of the fitting results in Fig. 7 to temperatures $T\geqslant 25$ K. At high

temperatures the ratios of the anisotropic exchange parameters remain practically unchanged, as expected from the linewidth ratios. Both interchain and intrachain anisotropic exchanges yield appreciable contributions. The relations between the anisotropic exchange parameters are $J_{xx}/J_{zz} = -0.63 \pm 0.02$ and $|A_{cc}/J_{zz}| = 0.64 \pm 0.02$ in the temperature range $120 \leqslant T \leqslant 300$ K. We note that the relation between the intrachain anisotropy parameters is almost the same as obtained for $LiCuVO_4$ at high temperatures, where $J_{xx}/J_{zz} = -0.57$ is found after adjusting the parameter values given in Ref. 15 with the condition $J_{xx}+J_{yy}+J_{zz}=0$.

The determination of the absolute values of the anisotropic exchange parameters in $CuGeO_3$ suffers from the uncertainty concerning the exchange frequency. From extrapolation of the linewidth data to $T \to \infty$ by means of Eq. (9) and using $\omega_{ex} \approx J/\hbar$, we obtained $|J_{zz}/k_B| = 3.2$ K. But this seems to be too large in comparison to $LiCuVO_4$ with the same chain structure. It may be possible that the next-nearest-neighbor exchange coupling J_c^{nnn}, which is appreciably large in $CuGeO_3$, reduces the exchange frequency. To our knowledge there does not exist any theoretical calculation for exchange narrowing, which takes into account the exchange interaction between both nearest and next nearest neighbors.

In $LiCuVO_4$ the absolute values of the anisotropic exchange parameters were independently obtained from the temperature dependence of the g values for the three crystal axes. In $CuGeO_3$ the g values do not exhibit a significant temperature dependence due to the weaker temperature dependence of the magnetic susceptibility in comparison to $LiCuVO_4$. Therefore, we assume that the parameter J_{zz} attains a value in $CuGeO_3$ similar to that in $LiCuVO_4$ because of the comparable bond structure within the Cu-O2 chains. Then it is possible to estimate from $|A_{cc}/J_{zz}| = 0.64$ that the interchain anisotropic exchange amounts $|A_{cc}|/k_B \approx 0.64 \times 1.22$ K ≈ 0.78 K. This value is in good agreement with the theoretical estimation given in Sec. II C and establishes the importance of the interchain anisotropic exchange for the linewidth in $CuGeO_3$.

On decreasing temperature the ratio $|A_{cc}/J_{zz}|$ gradually increases below 120 K up to approximately $|A_{cc}/J_{zz}| \approx 1 \pm 0.05$ below 40 K. The changes obtained for the intrachain exchange ratio J_{xx}/J_{zz} are weaker by a factor of 3 but similar to those in $|A_{cc}/J_{zz}|$. We can deduce that mainly the interchain exchange parameter $|A_{cc}/J_{zz}|$ accounts for the systematic changes of the linewidth ratios observed below 120 K, and therefore is connected to the lattice fluctuations in this temperature regime, which we discussed above. Finally, we can estimate the influence of the lattice changes on the interchain exchange, using the structural data given by Braden *et al.*[4] The Cu-O1 distance, which is relevant for the interchain exchange, decreases from $R = 2.7549$ Å at 295 K down to $R = 2.7295$ Å at 20 K. If one takes $(t_\pi/\Delta_\pi)^2 \propto R^{-6}$ in Eq. (8), then on lowering the temperature the variation of A_{cc} becomes about 10%, which is the correct order of magnitude. In addition, the strong sensibility of the exchange interaction to lattice deformations can be illustrated, e.g., for the superexchange in MnO, which was established as $J(R) \propto \exp(-15R/R_0)$ for the 90° Mn-O-Mn bond.[33] For small deviations δR from the equilibrium Mn-Mn distance R_0 the resulting change in J can be expanded as $\delta J/J(R_0) \approx -15\delta R/R_0$, which is about 15% for $\delta R/R_0 \approx 0.01$, in agreement with the present results for the anisotropic exchange in $CuGeO_3$.

V. CONCLUSIONS

We have performed detailed measurements of the angular and temperature dependence of the ESR linewidth in $CuGeO_3$, in order to clarify the controversially discussed question about the interaction, which is responsible for the line broadening in this compound. At high temperatures $T > J/k_B$ the anisotropy of the normalized linewidth is temperature independent, and can be well described in terms of symmetric anisotropic exchange only. The dominant contribution J_{zz} results from the intrachain ring exchange via the Cu-O2 ribbons. In addition we found an appreciable interchain contribution A_{cc}, which amounts about half of the intrachain anisotropic exchange. Based on previous results in $LiCuVO_4$, the experimental estimation of the interchain anisotropic exchange parameter practically coincides with our microscopic theoretical expectation $|A_{cc}| \approx 0.7$ K. At lower temperatures $T < J/k_B$ we observed a systematic change in the anisotropy of the normalized linewidth. As due to recent theoretical considerations of Oshikawa and Affleck the temperature dependence should be an isotropic function, if only one type of interaction governs the linewidth, we searched for possible reasons, which could affect the anisotropic exchange interaction. By comparison with experimental results from literature (e.g., neutron scattering) we found a clear coincidence of the linewidth behavior with the onset of lattice fluctuations for $T < J/k_B$, far above the spin-Peierls transition. From our evaluation we obtained a relative increase of the interchain contribution A_{cc} compared to the intrachain exchange J_{zz}. Hence, by means of electron-spin resonance, we found a quantitative estimate for the symmetric anisotropic exchange integrals in $CuGeO_3$. We suggested an empirical formula for the temperature dependence of the ESR linewidth with two characteristic parameters, which reflect the relevant interactions between the copper spins. Moreover we provide experimental evidence for structural fluctuations, which already start far above the spin-Peierls transition.

ACKNOWLEDGMENTS

We are strongly indebted to L. I. Leonyuk (M. V. Lomonosov Moscow State University), who prepared the samples. This work was supported by a joint project of Russian Foundation for Basic Research (RFBR) 01-02-04007 and Deutsche Forschungsgemeinschaft (DFG) 436 RUS 113/628, by the program Universities of Russia (Grant No. 01.01.023) and partially by BRHE REC007 and by the German Bundesministerium für Bildung und Forschung under the contract No. VDI/EKM 13N6917 and by DFG via SFB 484. One of the authors (V.G.) thanks the Forschungzentrum Jülich for continuous support of his studies.

APPENDIX: CALCULATION OF THE SECOND MOMENT

The second moment M_2 caused by the symmetric anisotropic exchange interaction can be calculated in coordinates with the z' axis along the external magnetic field in high-temperature approximation in analogy to Refs. 15 and 18 as

$$M_2 = 2\frac{S(S+1)}{3}\{f_1\cdot[2\lambda_{z'z'}-\lambda_{x'x'}-\lambda_{y'y'}]^2 + 10f_2\cdot[\lambda_{x'z'}^2+\lambda_{y'z'}^2] + f_3\cdot[(\lambda_{x'x'}-\lambda_{y'y'})^2+4\lambda_{x'y'}^2]\}. \quad \text{(A1)}$$

The factor 2 appears due to the summation over nearest neighbors, f_1, f_2, and f_3 denote the spectral density functions as introduced by Pilawa.[13] The factor f_1 corresponds to the secular, the factors f_2 and f_3 to the non-secular parts of the second moment, respectively. The values $\lambda_{\alpha'\beta'}$ are exchange-tensor components in the coordinates with $z'\|H$, they can be expressed via the intrinsic exchange parameters J_{aa}, J_{bb}, J_{cc} for the intrachain exchange ($M_2^{(1,2)}$) by the following transformation formulas

$$(2\lambda_{z'z'}-\lambda_{x'x'}-\lambda_{y'y'})^2 = \{J_{cc}(3\cos^2\beta-1)+J_{aa}(3\sin^2\beta\cos^2\alpha-1) + J_{bb}(3\sin^2\beta\sin^2\alpha-1)+3J_{ab}\sin^2\beta\sin 2\alpha\}^2, \quad \text{(A2)}$$

$$\lambda_{x'z'}^2+\lambda_{y'z'}^2 = \{(J_{aa}\cos^2\alpha+J_{bb}\sin^2\alpha-J_{cc}+J_{ab}\sin 2\alpha)\cos\beta\sin\beta\}^2 + \{(J_{bb}-J_{aa})\sin\beta\cos\alpha\sin\alpha+J_{ab}\sin\beta\cos 2\alpha\}^2, \quad \text{(A3)}$$

$$(\lambda_{x'x'}-\lambda_{y'y'})^2+4\lambda_{x'y'}^2 = 4\{(J_{bb}-J_{aa})\cos\beta\sin\alpha\cos\alpha+J_{ab}\cos\beta\cos 2\alpha\}^2 + \{J_{aa}(\cos^2\beta\cos^2\alpha-\sin^2\alpha)+J_{bb}(\cos^2\beta\sin^2\alpha - \cos^2\alpha)+J_{cc}\sin^2\beta+J_{ab}\sin 2\alpha(\cos^2\beta+1)\}^2, \quad \text{(A4)}$$

where

$$\cos\alpha = \frac{A}{\sqrt{A^2+B^2}},$$

$$\cos\beta = \frac{C}{\sqrt{A^2+B^2+C^2}},$$

with

$$A = g_{aa}\sin\theta\cos\phi+g_{ab}\sin\theta\sin\phi,$$

$$B = g_{ba}\sin\theta\cos\phi+g_{bb}\sin\theta\sin\phi,$$

$$C = g_{cc}\cos\theta.$$

The angles θ and ϕ define the magnetic field orientation with respect to the crystallographic axes. The g tensor in crystallographic coordinates is obtained from the g tensor in local coordinates by

$$g_{aa} = g_{zz}\sin^2\gamma+g_{xx}\cos^2\gamma,$$

$$g_{bb} = g_{zz}\cos^2\gamma+g_{xx}\sin^2\gamma,$$

$$g_{cc} = g_{yy},$$

$$g_{ab} = g_{ba} = \pm(g_{zz}-g_{xx})\sin\gamma\cos\gamma, \quad \text{(A5)}$$

where the angle γ denotes the angle between the crystallographic a axis and Cu-O2 ribbon (see Fig. 1) and $g_{zz}=2.33$, $g_{xx}=2.03$, and $g_{yy}=2.04$. Plus and minus sign refer to the two inequivalent Cu places. The same equations hold for the transformation of the anisotropic exchange tensor from local (J_{xx}, J_{yy}, J_{zz}) into crystallographic coordinates. The interchain exchange contribution ($M_2^{\perp}$) is analogously expressed via the parameter A_{cc}.

*Electronic address: Hans-Albrecht.Krug@physik.uni-augsburg.de

[1] M. Hase, I. Terasaki, and K. Uchinokura, Phys. Rev. Lett. **70**, 3651 (1993).
[2] J.P. Boucher and L.P. Regnault, J. Phys. I **6**, 1939 (1996).
[3] H. Völenkle, A. Wittmann, and H. Nowotny, Monatsh. Chem. **98**, 1352 (1967).
[4] M. Braden, G. Wilkendorf, J. Lorenzana, M. Ain, G.J. McIntyre, M. Behruzi, G. Heger, G. Dhalenne, and A. Revcolevschi, Phys. Rev. B **54**, 1105 (1996).
[5] M. Hidaka, M. Hatae, I. Yamada, M. Nishi, and J. Akimitsu, J. Phys.: Condens. Matter **9**, 809 (1997).
[6] M. Nishi, O. Fujita, and J. Akimitsu, Phys. Rev. B **50**, 6508 (1994).
[7] J. Riera and A. Dobry, Phys. Rev. B **51**, 16 098 (1995).
[8] S. Oseroff, S.-W. Cheong, A. Fondado, B. Aktas, and Z. Fisk, J. Appl. Phys. **75**, 6819 (1994).
[9] H. Ohta, S. Imagawa, H. Ushiroyama, M. Motokawa, O. Fujita, and J. Akimitsu, J. Phys. Soc. Jpn. **63**, 2870 (1996).
[10] I.M. Honda, T. Shibata, K. Kindo, S. Sugai, T. Takeuchi, and H. Hori, J. Phys. Soc. Jpn. **65**, 691 (1996).
[11] A.I. Smirnov, V.N. Glazkov, L.I. Leonyuk, A.G. Vetkin, and R.M. Eremina, Pis'ma Zh. Éksp. Teor. Fiz. **114**, 1876 (1998) [JETP **87**, 1019 (1998)].
[12] I. Yamada, M. Nishi, and J. Akimitsu, J. Phys.: Condens. Matter **8**, 2625 (1996); I. Yamada, J. Phys. Soc. Jpn. **65**, 3408 (1996).
[13] B. Pilawa, J. Phys.: Condens. Matter **9**, 3779 (1997).
[14] M. Oshikawa and I. Affleck, Phys. Rev. B **65**, 134410 (2002).
[15] H.-A. Krug von Nidda, L.E. Svistov, M.V. Eremin, R.M. Eremina, A. Loidl, V. Kataev, A. Validov, A. Prokofiev, and W. Assmus, Phys. Rev. B **65**, 134445 (2002).

[16] R. Kubo and K. Tomita, J. Phys. Soc. Jpn. **9**, 888 (1954).
[17] P.W. Anderson, J. Phys. Soc. Jpn. **9**, 316 (1954).
[18] Z.G. Soos, K.T. McGregor, T.T.P. Cheung, and A.J. Silverstein, Phys. Rev. B **16**, 3036 (1977).
[19] A. Abragam, *The Principles of Nuclear Magnetism* (Clarendon Press, Oxford, 1961).
[20] A. Bencini and D. Gatteschi, *Electron Paramagnetic Resonance Spectroscopy of Exchange Coupled System* (Springer-Verlag, Berlin, 1990).
[21] D. Khomskii, W. Geertsma, and M. Mostovoy, Proc. of the LT21 [Czech. J. Phys. **46**, 3043 (1996)].
[22] W. Geertsma and D. Khomskii, Phys. Rev. B **54**, 3011 (1996).
[23] S. Tornow, O. Entin-Wohlman, and A. Aharony, Phys. Rev. B **60**, 10 206 (1999).
[24] T. Moriya, Phys. Rev. **120**, 91 (1960).
[25] M.V. Eremin, Theory of exchange interaction of magnetic ions in dielectrics (in Russian), in *Spectroscopy of Crystals*, edited by A.A. Koplyanskii (Nauka, Leningrad, 1986), pp. 150–172.
[26] A. Abragam and B. Bleaney, *Electron Paramagnetic Resonance of Transition Ions* (Clarendon Press, Oxford, 1970).
[27] R.E. Walstedt and S.-W. Cheong, Phys. Rev. B **64**, 014404 (2001).
[28] H. Eskes, L.H. Tjeng, and G.A. Sawatzky, Phys. Rev. B **41**, 288 (1990).
[29] M.S. Hybertsen, E.B. Stechel, W.M.C. Foulkes, and M. Schluter, Phys. Rev. B **45**, 10 032 (1992).
[30] M. Braden, B. Hennion, W. Reichardt, G. Dhalenne, and A. Revcolevschi, Phys. Rev. Lett. **80**, 3634 (1998).
[31] C.H. Chen and S-W. Cheong, Phys. Rev. B **51**, 6777 (1995).
[32] G. Quirion, F.S. Razavi, B. Dumoulin, M. Poirier, A. Revcolevschi, and G. Dhalenne, Phys. Rev. B **58**, 882 (1998).
[33] J. Owen and E.A. Harris, in *Electron Paramagnetic Resonance*, edited by S. Geschwind (Plenum Press, New York, 1972).